Identification of cell populations necessary for leaf-to-leaf electrical signaling in a wounded plant

Chi Tam Nguyen[a,1], Andrzej Kurenda[a,1], Stéphanie Stolz[a], Aurore Chételat[a], and Edward E. Farmer[a,2]

[a]Department of Plant Molecular Biology, University of Lausanne, CH-1015 Lausanne, Switzerland

Edited by Julian I. Schroeder, Cell and Developmental Biology Section, Division of Biological Sciences, University of California, San Diego, La Jolla, CA, and approved August 23, 2018 (received for review April 24, 2018)

The identity of the cell files necessary for the leaf-to-leaf transmission of wound signals plants has been debated for decades. In *Arabidopsis*, wounding initiates the glutamate receptor-like (GLR)–dependent propagation of membrane depolarizations that lead to defense gene activation. Using a vein extraction procedure we found pools of GLR-fusion proteins in endomembranes in phloem sieve elements and/or in xylem contact cells. Strikingly, only double mutants that eliminated GLRs from both of these spatially separated cell types strongly attenuated leaf-to-leaf electrical signaling. *glr3.3* mutants were also compromised in their defense against herbivores. Since wounding is known to cause increases in cytosolic calcium, we monitored electrical signals and Ca^{2+} transients simultaneously. This revealed that wound-induced membrane depolarizations in the wild-type preceded cytosolic Ca^{2+} maxima. The axial and radial distributions of calcium fluxes were differentially affected in each *glr* mutant. Resolving a debate over which cell types are necessary for electrical signaling between leaves, we show that phloem sieve elements and xylem contact cells function together in this process.

jasmonate | Ricca's factor | xylem | phloem | calcium

Organ-to-organ electrical signaling is a highly conserved feature of land plants. For example, wound-induced electrical signals known as "slow wave potentials" (SWPs; otherwise known as "variation potentials") have been found in numerous species (1, 2). In *Arabidopsis thaliana*, severe damage triggers electrical activity that propagates from leaf to leaf with apparent velocities in the centimeter-per-minute range. These events are characterized by rapid (<2 s) and massive (>50 mV) membrane depolarizations followed by slow (>5 min) repolarizations (3); each is a feature characteristic of SWPs (4, 5). At their destination in leaves distal to wounds, and strongly suggesting roles in plant defense, membrane depolarization in *Arabidopsis* stimulates the accumulation of the potent lipidic regulator jasmonate (JA). To initiate multiple defense responses, JA mediates the destruction of components of transcriptional repressor complexes to enhance gene expression (6–8). JA synthesis initiates this process. When a leaf is wounded, electrical signals travel to distal leaves to first trigger JA or JA precursor synthesis in a small population of cells known as xylem contact cells (9, 10). These cells then export JA precursors and/or JA to surrounding tissues (10). Which cells are necessary to conduct electrical signals to these distal sites of JA production?

Despite a debate that is decades old and that emerged in large part from studies of the sensitive plant *Mimosa pudica* (e.g., ref. 11), a consensus regarding which cell populations are necessary for organ-to-organ electrical signaling in plants has never been reached. On the one hand, the xylem has been proposed to play an essential, if not exclusive, role in this phenomenon. For example, a long-standing theory is that chemical elicitors ("Ricca's factor") drawn over long distances through the xylem activate distal movement responses in *M. pudica* (12). This mechanism is thought to occur in other species (e.g., ref. 13). Alternatively, hydraulic signals in the xylem have been proposed to underlie SWP propagation (14). In each of these cases, dead xylem vessels rather than the living cells that surround them have been implicated in the events leading to long-distance propagation of electrical signals. On other hand, evidence going back to the 1920s supports roles of the phloem in leaf-to-leaf electrical signaling (15–18), and wound-response electrical signals have been detected directly in sieve elements (19). Moreover, wounding initiates systemic calcium fluxes in *Arabidopsis* (e.g., ref. 20), and phloem cells have been implicated repeatedly in wound-response calcium signaling (17). Finally, both phloem and xylem-associated cells in *M. pudica* were found to be highly excitable (21), raising the possibility that both cell populations operate in the leaf movement response.

To address the question of which cell types are necessary for organ-to-organ electrical signaling in *Arabidopsis*, we based our approach on *GLUTAMATE RECEPTOR-LIKE* (*GLR*) genes (*GLR3.1*, *-3.2*, *-3.3*, and *-3.6*) that were recently found to function in this process (3). Functional GLR protein fusions were generated from three of these genes to identify the exact cell populations involved in SWP propagation. Then, based on the fact that wounding induces local and distal cytosolic calcium transients (20, 22), we developed a method to simultaneously monitor electrical activity and calcium levels. Our results build a cell-level understanding of the SWP.

Results

GLR Function in Membrane Repolarization and Defense Against Herbivores. The *glr3.3 glr3.6* double mutant attenuates wound-activated electrical signal propagation between leaves (3). To characterize additional genetic interactions and thereby define a

Significance

Numerous modes of long-distance electrical signaling exist in nature. The best known of these, axonal conduction, requires one primary cell population, i.e., neurons. In contrast, the cell types that mediate leaf-to-leaf electrical signaling in wounded plants have not been defined rigorously. Using genetic approaches, we find that two distinct populations of cells in the vasculature matrix are needed to perform this function. Surprisingly, these cells do not contact each other directly. As we further defined the plant wound response, we found that wound-induced membrane depolarizations preceded large intravasculature calcium fluxes. We reveal a two-cell-type mode of electrical signaling in leaves and discuss parallels and differences in electrical signaling outside the plant kingdom.

Author contributions: C.T.N., A.K., and E.E.F. designed research; C.T.N., A.K., S.S., and A.C. performed research; C.T.N., A.K., and E.E.F. analyzed data; and C.T.N., A.K., and E.E.F. wrote the paper.

The authors declare no conflict of interest.

This article is a PNAS Direct Submission.

[1]C.T.N. and A.K. contributed equally to the work.

[2]To whom correspondence should be addressed. Email: edward.farmer@unil.ch.

This article contains supporting information online at www.pnas.org/lookup/suppl/doi:10.1073/pnas.1807049115/-/DCSupplemental.

Published online September 18, 2018.

minimum set of GLRs for defense bioassays and tissue localization, we stimulated *glr* single mutants with a laser that produced highly reproducible wounds at the petiole/lamina junction of leaf 8. Signals were captured with noninvasive surface electrodes placed on distal undamaged leaf 13 that shares strong vascular connections with leaf 8 (3). Under these conditions, mutations in *GLR3.1*, *-3.2*, *-3.3*, and *-3.6* reduced surface potential duration in distal leaf 13 without strongly affecting signal amplitude (Fig. 1*A*). Next, double mutants were generated. Fig. 1*B* shows that mutants harboring the *glr3.2* mutation had relatively weak effects on surface potentials, so this gene was eliminated from further analysis. In contrast, double mutants carrying the *glr3.3* mutation (*glr3.1 glr3.3* and *glr3.3 glr3.6*) eliminated laser-induced depolarizations recorded from distal leaf 13. We conclude that the GLRs act as regulators of membrane potential in wounded plants. To test the defenses of *glr* mutants, plants were challenged with larvae of *Spodoptera littoralis*. Among the single mutants tested, the insects gained weight most rapidly on *glr3.3* (Fig. 1*C*). The larvae gained weight faster on the double mutants than on the wild type (WT) (Fig. 1*D*).

GLR Expression in the Primary Vasculature. Having found that both *glr3.1 glr3.3* and *glr3.3 glr3.6* double mutants attenuate electrical signaling to distal leaves, we undertook to identify sites of expression of *GLR3.1*, *-3.3*, and *-3.6*. For this, a three-step approach was taken to localize the GLRs in adult-phase leaves of the same age as used for surface potential measurements and bioassays. First, to look at overall expression in whole leaves, *GLR* promoters fused to the reporter gene β-glucuronidase (GUS). *GLR3.1* promoter activity was detected in primary and secondary veins, but expression was not detectable in tertiary veins (Fig. 2*A*). Reporter activity for *GLR3.3* (Fig. 2*B*) was observed in primary, secondary, and tertiary veins and in the epidermis in trichome base cells and in guard cells (Fig. 2 *C* and *D*). *GLR3.6* promoter activity was observed in all three vein orders (Fig. 2*E*). In summary, all three *GLR* promoters were active in the primary and secondary veins. We focused on the primary vein.

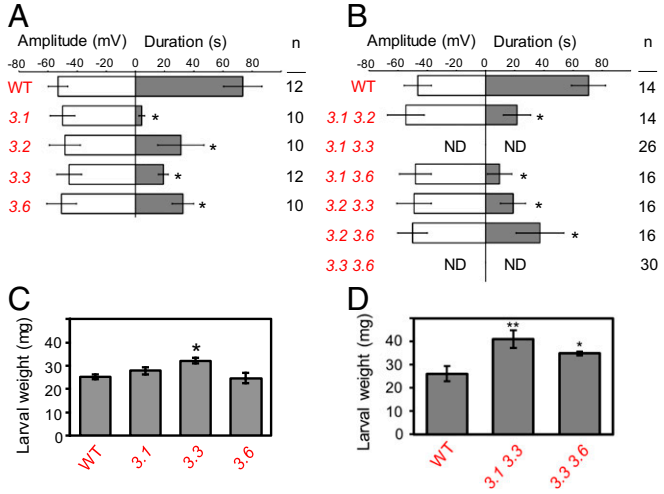

Fig. 1. Impaired electrical signal propagation and accelerated insect growth on double mutants carrying the *glr3.3* mutation. (*A*) Surface potential changes in leaf 13 in *glr* single mutants that were laser-wounded on leaf 8. (*B*) Surface potentials in *glr* double mutants. *n* = number of technical replicates. ND, signal not detectable. Genetic backgrounds are indicated in red. (*C*) Weight of *S. littoralis* larvae grown for 12 d on the WT or on *glr* single mutants. (*D*) Weight of larvae grown for 12 d on the WT or on *glr* double mutants. Data shown are means ± SD. Asterisks indicate significant differences to the WT. Student *t* test: $*P < 0.01$; $**P < 0.001$.

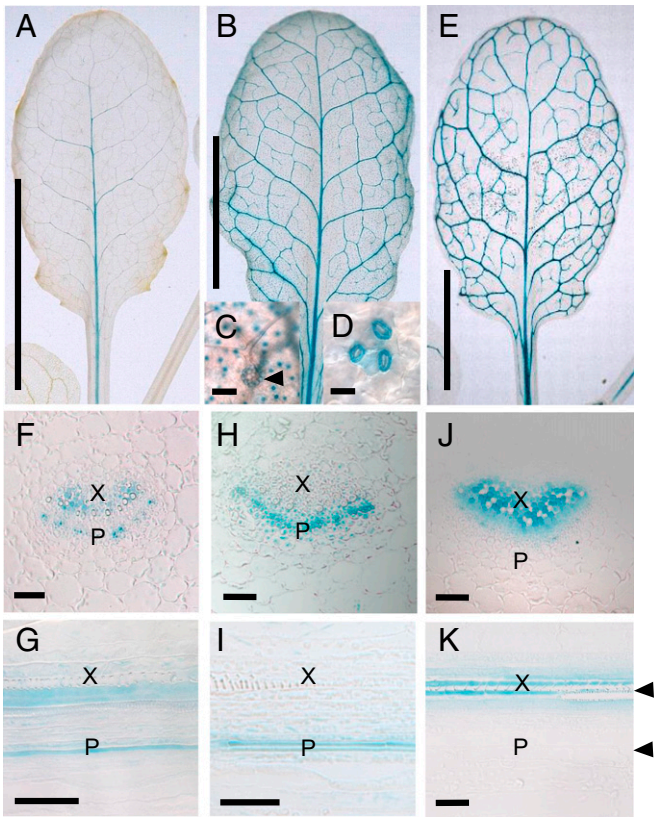

Fig. 2. *GLR* promoter activity associated with the vasculature. (*A*) GUS staining pattern for a *GLR3.1pro::GUS* transcriptional reporter in an expanded leaf from a 4-wk-old rosette. (Scale bar: 1 cm.) (*B*) GUS staining pattern for a *GLR3.3pro::GUS* transcriptional reporter. (Scale bar: 0.5 cm.) (*C*) GUS staining in trichome base cells (arrowhead). (Scale bar: 100 μm.) (*D*) Stained guard cells. (Scale bar: 10 μm.) (*E*) Promoter activity of a *GLR3.6pro::GUS* transcriptional reporter. (Scale bar: 0.5 cm.) (*F*) Transversal section from a leaf expressing a translational *GLR3.1pro::GLR3.1-GUS* fusion. (*G*) Longitudinal petiole section from a *GLR3.1pro::GLR3.1-GUS* plant. (*H*) Transversal petiole cross-section from a translational *GLR3.3pro::GLR3.3-GUS* fusion. (*I*) Longitudinal petiole section from a *GLR3.3pro::GLR3.3-GUS* plant. (*J*) Transversal petiole cross-section from a *GLR3.6pro::GLR3.6$_{cDNA}$-GUS* translational reporter. (*K*) Longitudinal petiole section from a *GLR3.6pro::GLR3.6$_{cDNA}$-GUS* plant. (Scale bars, *F*–*K*: 50 μm.) X, xylem region; P, phloem region—both indicated by arrowheads.

As a second step, translational *GLRpro::GLR-GUS* fusions were produced. GLR3.1-GUS was detected in or near xylem contact cells (XCCs) and, at a low level, in the phloem region (Fig. 2 *F* and *G*). GLR3.3-GUS was most strongly expressed in the phloem region (Fig. 2 *H* and *I*), and GLR3.6-GUS localized to the xylem region (Fig. 2 *J* and *K*). These results indicated that the GLRs were expressed in core vascular cells in the primary vein.

With the goal of determining the identity of these cells, genomic *GLR* clones were coupled to a single fluorescent VENUS tag and used to complement the cognate mutant backgrounds (*SI Appendix*, Table S1). Gaining facile optical access to the GLRs in roots was possible, but this was not considered appropriate since electrical signaling in roots and shoots differs markedly (10). However, accessing core vascular cells in the primary veins proved difficult. Therefore, a rapid midvein extraction procedure was developed to overcome this obstacle. The procedure does not require chemical treatments or protoplasting. Primary veins were extracted from expanded leaves (Fig. 3*A*). Inspection of the extracted veins showed that core vascular cells remained intact (Fig. 3*B*).

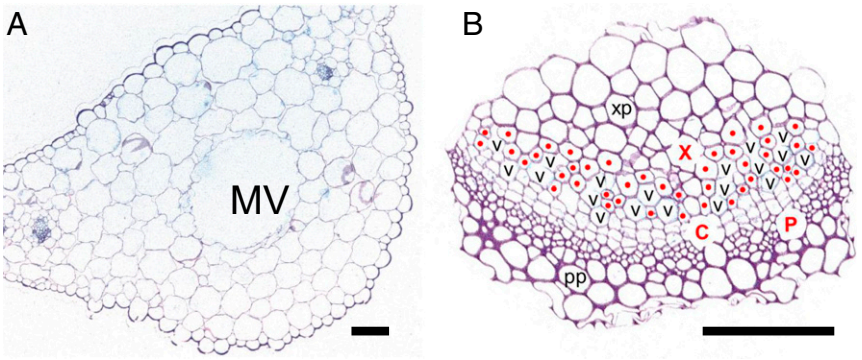

Fig. 3. Rapid midvein extraction from a 5-wk-old plant. (*A*) Transversal section near the leaf-petiole junction showing zone left by midvein (MV) after its rapid removal. (Scale bar: 30 μm.) (*B*) Transversal section of an extracted midvein. C, cambium region; P, phloem region; pp, phloem parenchyma; V, vessel; X, xylem region; xp, xylem parenchyma; red dots indicate contact cells. (Scale bar: 30 μm.) The sections were stained with 0.1% (wt/vol) toluidine blue in water.

Extracted midveins were either fixed and cleared directly (23, 24), subject to brief protoplasting to remove outer cell layers of parenchymal cells, or observed directly. Functional GLR3.1-VENUS fusion proteins localized primarily to XCCs (Fig. 4 *A* and *B*), and, in agreement with observation of the GLR3.1-GUS translational fusion (Fig. 2 *G* and *F*), a second low abundance pool of GLR3.1-VENUS was detected occasionally in phloem sieve elements (SEs) (*SI Appendix*, Fig. S1). In the root division zone, *GLR3.3* is expressed in a wide range of cell types (25). In the leaf primary vasculature, we found that GLR3.3-VENUS localized primarily to SEs (Fig. 4*C*). Sieve plate pores have been implicated as sites of ion channel expression (26). To observe sieve plates, isolated veins were subjected to complete protoplasting. In these samples, GLR3.3-VENUS was observed at the sieve plate periphery (*SI Appendix*, Fig. S2). Next, we examined GLR3.6-VENUS localization. Rapid vein extraction followed immediately by clearing and fixing revealed that GLR3.6-VENUS localized to xylem contact cells (*SI Appendix*, Fig. S3). When partial protoplasting was used to remove outer parenchymal cells of freshly extracted veins, the VENUS signal again located to large organelles within contact cells (Fig. 4*D*). In summary, phloem SEs and XCCs separated by the cambial region (*SI Appendix*, Fig. S4) contribute to propagation of the SWP from leaf to leaf.

Next, we assessed the major subcellular localizations of the GLR-VENUS fusion proteins. In the case of GLR3.1-VENUS, partial protoplasting to remove outer vascular cell layers was necessary to visualize the VENUS tag. GLR3.1 was found in punctate structures that resembled endoplasmic reticulum (ER). GLR3.1-VENUS was therefore introgressed into the red fluorescent protein (RFP)–ER marker line WAVE 6R (27). The fusion proteins and the ER marker proteins were found to colocalize in XCCs (*SI Appendix*, Fig. S5 *A–C*) and in the phloem SEs (*SI Appendix*, Fig. S5 *D–F*). In the case of GLR3.3-VENUS, punctate structures resembling ER were seen, and GLR3.3-VENUS was found to colocalize with the WAVE 6R ER marker (*SI Appendix*, Fig. S5 *G–I*). Crossing GLR3.6-VENUS into the WAVE 9R marker line that tags vacuole membranes (27) revealed vacuolar colocalization of the two fluorescent tags (*SI Appendix*, Fig. S5 *J–O*).

Membrane Depolarization Maxima Precede Wound-Associated Cytosolic Calcium Maxima. GLR3.4 and GLR3.1/GLR3.5 heteromers form calcium-permeable channels (28, 29). Also, several GLRs control Ca^{2+} levels in pollen tubes (30), and *Physcomitrella* GLRs are Ca^{2+}-permeable channels (31). Furthermore, cytosolic Ca^{2+} levels increase in seconds in tissues proximal to wounds (22). With the goal of defining the temporal and spatial relationships of SWPs and Ca^{2+} signals we employed the GCaMP3 reporter (32) that is known to detect Ca^{2+} fluxes in leaves (33). The presence of this protein expressed from the *UBIQUITIN 10* promoter did not strongly affect electrical activity after wounding (*SI Appendix*, Fig. S6). Additionally, each GCaMP3-expressing line was tested for its response to a nonwounding application of ice-cold water. The reporter responded similarly in each case (*SI Appendix*, Fig. S7). Experiments began with analysis of *Pieris brassicae* feeding on the WT background. For these initial analyses, WT plants at the 2-wk growth stage were chosen since calcium signals in veins are clearly demarcated by that age. As they fed, the larvae triggered vein-associated fluorescence (Fig. 5*A* and Movie S1). The apparent velocities of Ca^{2+} waves elicited in leaves distal to caterpillar feeding sites were greater in the petiole than in the laminal midvein and faster in the primary vein than in secondary or tertiary veins (Fig. 5*B*).

Since the three GLRs that we studied all localized to the primary vasculature, we tested whether the midvein alone was

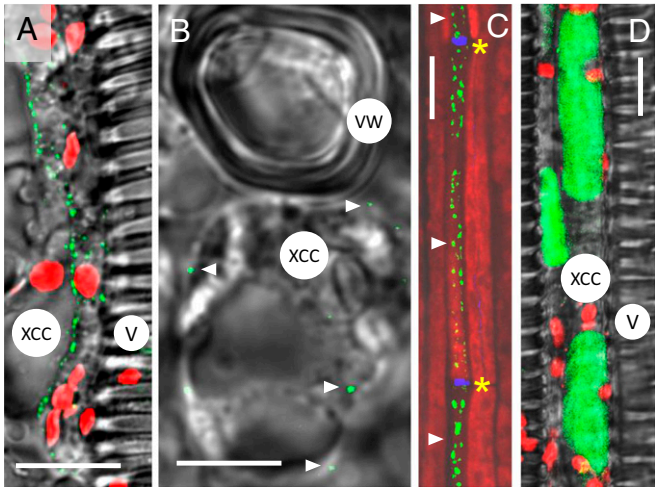

Fig. 4. GLR-VENUS expression in the primary leaf vein. (*A*) GLR3.1-VENUS localization (green) in contact cells; longitudinal section. Red is chlorophyll fluorescence. V, xylem vessel; XCC, xylem contact cell. (Scale bar: 10 μm.) (*B*) GLR3.1-VENUS (arrowheads) in a contact cell; transversal section. VW, vessel wall. (Scale bar: 5 μm.) (*C*) GLR3.3-VENUS localization (green) in SEs. The sample was fixed, cleared, and then stained with aniline blue and propidium iodide (red). Arrowheads indicate sieve cells; asterisks indicate aniline blue-stained sieve plates. (Scale bar: 10 μm.) (*D*) GLR3.6-VENUS (green) in xylem contact cells. Red is chlorophyll fluorescence. (Scale bar: 10 μm.) For *A*, *B*, and *D* mild protoplasting of freshly isolated veins in 500 mM sorbitol (*A* and *B*) or 100 mM sorbitol (*D*) was used to remove large peripheral parenchyma cells. For *C*, an isolated primary vein was fixed and cleared before staining.

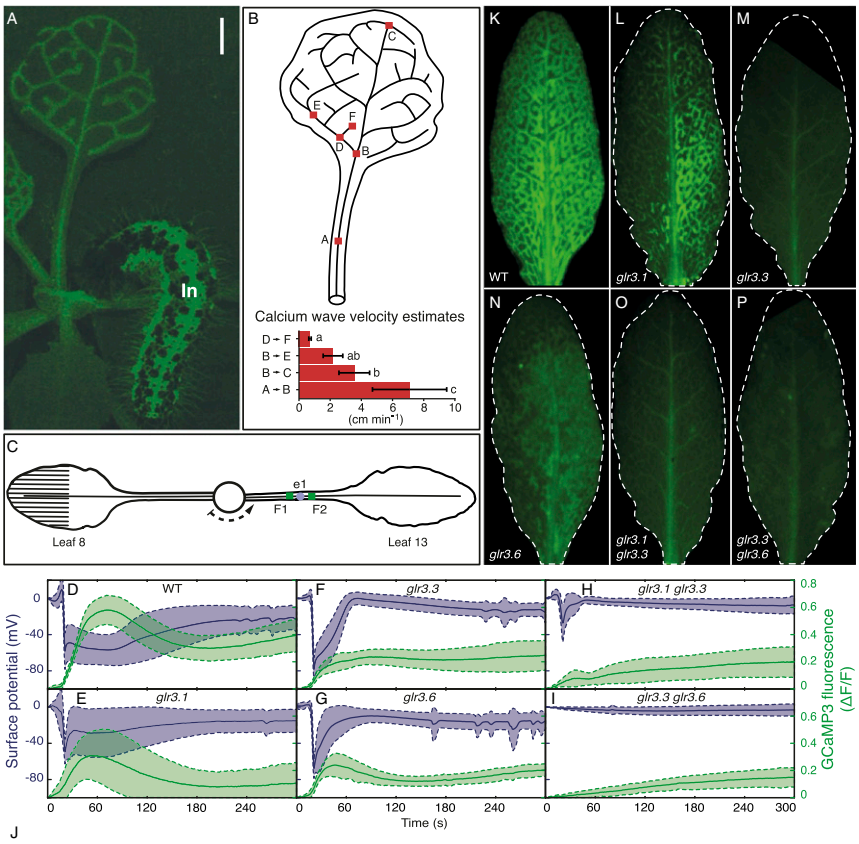

Genotype	Amplitude at e1 (ΔF/F or mV)		Duration at e1 (s)		Velocity (cm min^{-1}) to e1		Maximal slope at e1 (ΔF/F s^{-1} or mV s^{-1})	
	Ca^{2+} wave	Surface potential	Ca^{2+} wave	Surface potential	Ca^{2+} wave	Surface potential	Ca^{2+} wave	Surface potential
WT	0.58±0.1^{a}	-75.9±7^{ab}	134±36^{a}	223±125^{a}	9.27±3.5^{a}	9.76±2.9^{a}	0.018±0.004^{a}	-49.8±15^{a}
glr3.1	0.33±0.19^{b}	-59.6±10^{ac}	85.1±29^{b}	40.2±60^{b}	5.1±1.5^{b}	5.44±2.1^{b}	0.012±0.005^{bc}	-26.2±11^{b}
glr3.3	0.27±0.08^{b}	-84.3±18^{b}	113±57^{ab}	23±11^{b}	6.02±3.4^{ab}	5.96±3.4^{ab}	0.008±0.003^{c}	-36.8±16^{ab}
glr3.6	0.26±0.07^{b}	-66.4±18^{abc}	76±19^{b}	15±10^{b}	7.4±2.1^{ab}	7.25±2.2^{ab}	0.013±0.003^{b}	-37.5±16^{ab}
glr3.1 glr3.3	0.2±0.1^{b}	-50.7±8^{c}	24±3^{c}	10.8±7^{b}	6.86±1.9^{ab}	6.73±2^{ab}	0.003±0.003^{d}	-18.4±8^{b}
glr3.3 glr3.6	-	-	-	-	-	-	-	-

Fig. 5. Wound-induced cytosolic Ca^{2+} levels in WT and *glr* mutants. (*A*) *P. brassicae* feeding-induced *UBQ10pro*::GCaMP3 fluorescence in a 2-wk-old plant. The frame is from Movie S1. In, insect. (Scale bar: 1 mm.) (*B*) Ca^{2+} wave velocity estimates between points indicated with red squares recorded during *P. brassicae* feeding. Statistical significance was calculated using one-way ANOVA and Tukey's multiple comparisons test; means ± SD (n = 4). (*C*) Setup for simultaneous surface potential and GCaMP3 fluorescence monitoring in the petiole of leaf 13. Arrow indicates that leaf 13 is rotated relative to its natural position with respect to leaf 8. A crush wound is indicated on leaf 8. F1 and F2, positions of GCaMP3 fluorescence monitoring. Signals from F1 and F2 were averaged for comparison with electrical activity measured at e1. (*D–I*) Results of simultaneous monitoring of surface potentials and GCaMP3 fluorescence in leaf 13 after wounding leaf 8. Lines (purple, electrical activity; green, GCaMP3 fluorescence) are means; envelopes are SDs (n = 7–10 plants per genotype). (*J*) Quantitative data for surface potential changes and GCaMP3 fluorescence in leaf 13 of the wounded WT and *glr* mutants. Statistical significance was calculated using one-way ANOVA and Tukey's multiple comparisons test. Genotypes for which responses do not differ significantly are represented with the same letter. (*K–P*) Maximum induced GCaMP3 fluorescence in the laminae of leaf 13 of 5-wk-old plants after crush-wounding leaf 8. Dashed white lines indicate the outline of the leaf used. Note that in *M* and *P* the leaf tip was out of the field of view of the fluorescence camera.

sufficient for passage of the wound signal to a distal leaf. To do this, extravascular tissues surrounding the primary vasculature of leaf 13 were removed before crush-wounding leaf 8. In response to damage, both electrical signals and increases in GCaMP3 fluorescence were detected distal to the exposed vein. However, the apparent velocity of the Ca^{2+} signal was reduced by ~60% as it traversed the exposed vein (Movie S2). Next, we investigated the spatial distribution of wound-stimulated GCaMP3 fluorescence. When leaf 8 of the WT was wounded, SWPs spread to certain distal leaves (e.g., leaf 13) but not to leaf 9 (3). To investigate whether this was also the case for Ca^{2+} signals, leaf 8 was wounded, and GCaMP3 fluorescence was monitored in leaves 9 and 13. Only leaf 13 displayed strong fluorescence increases in these experiments (*SI Appendix*, Fig. S8).

In relation to the WT, Ca^{2+} signals in leaf 13 were affected in all *glr* mutant backgrounds (*SI Appendix*, Fig. S9*A* and Movie S3). With the possible exception of *glr3.1*, all mutants displayed reduced Ca^{2+} signal in wounded leaf 8 (*SI Appendix*, Fig. S9*B*). In both double mutants, the GCaMP3 signals reaching leaf 13 were weak (*SI Appendix*, Fig. S10). What is the temporal relationship between wound-activated membrane depolarization and wound-induced GCaMP3 fluorescence? To assess this, these outputs were monitored simultaneously as shown in Fig. 5*C*. In the WT, both events were initiated after wounding within a similar time frame. After the rapid decrease in surface potential,

the slower recovery phase correlated with the formation and diminution of the Ca^{2+} peak (Fig. 5*D* and Movie S2). Each *glr* mutant differentially reduced the amplitude of the Ca^{2+} wave in leaf 13. The *glr3.3* mutation, for example, attenuated peak GCaMP3 fluorescence in petioles more strongly than did the *glr3.1* or *glr3.6* mutations (Fig. 5 *E–G*). Finally, in response to crush wounding, short duration surface potential changes were sometimes detected in *glr3.1 glr3.3*, but not in *glr3.3 glr3.6* (Fig. 5 *H* and *I*). Fig. 5 *D–I* and further analyses (Fig. 5*J*) showed that Ca^{2+} wave amplitudes correlated with electrical signal durations, and the apparent axial velocities of the two signals were similar.

Spatial analyses of GCaMP3 fluorescence after wounding revealed mutant-specific features (Fig. 5 *K–P*). The Ca^{2+} signal in leaf 13 of *glr3.1* was often restricted to one leaf half-proximal to wounded leaf 8 (Fig. 5*L*). In *glr3.3*, the Ca^{2+} signal in this leaf was weaker and exclusively vascular compared with the signal from the WT, *glr3.1*, and *glr3.6* in which some perivascular GCaMP3 fluorescence was visible. Given the possible asymmetry in the Ca^{2+} signal in leaf 13 of *glr3.1* (Fig. 5*L*), we examined this mutant and found that the half of leaf 13 proximal to leaf 8 often produced stronger GCaMP3 fluorescence than did the leaf half distal to leaf 8 (*SI Appendix*, Fig. S11). This effect of the *glr3.1* mutation on the radial calcium signal is consistent with a different contribution to SWP propagation for GLR3.1 compared with GLR3.3 and GLR3.6.

Discussion

Fast nervous conduction in animals evolved under strong selection from predators (34). Here we argue that pressures from herbivores have led to the evolution of leaf-to-leaf electrical signaling in plants. It has long been known that mechanostimulation of the sensitive plant *M. pudica* leads to membrane depolarization that results in visual crypsis whereby leaves effectively disappear from view (15). Additionally, electrical signaling correlated with the production of defense-related proteinase inhibitors in tomato (35). More recently, genetic analysis revealed that electrical signaling stimulates the synthesis of the defense hormone JA in leaves distal to wounds. *GLR3.3* is known to be necessary for full resistance of *Arabidopsis* to a fungus (36). Do the GLRs that participate in electrical signal propagation contribute to defense against chewing herbivores? This appears to be the case since the bioassays conducted in the present work (Fig. 1) show that larvae grown on plants carrying the *glr3.3* mutation gain weight more rapidly than they do on the WT. These findings underscore the importance of the GLR3.3 gene in defense activation and strongly implicate the phloem in signaling leading to activation of defense against herbivores. Together, our results support the hypothesis that a primary role of SWP in plants is to activate defenses in tissues distal to wounds. Defense-related electrical signaling is therefore common to both the plant and animal kingdoms.

Insights into Electrical Signaling. A key finding of our study was that, in the *Arabidopsis* SWP, two highly distinct vascular cell populations act to propagate wound signals from leaf to leaf. Without inactivating XCC-expressed GLR3.6 or GLR3.1 in the *glr3.1 glr3.3* and the *glr3.3 glr3.6* double mutants, *glr3.3* alone does not fully eliminate electrical signals in distal leaves. XCCs are perfectly placed to sense changes in solute composition or in water potential or water tension that may occur if xylem vessels are ruptured. Interestingly, natural variants of *GLR3.6* in *Arabidopsis halleri* are found in environments that may affect plant hydration (37), and roles of GLRs in water pressure/tension sensing have been proposed (4). Strikingly, GLR3.6 shares a similar expression domain to lipoxygenase 6 (LOX6), which is necessary for the rapid synthesis of JA in leaves distal to wounds (9, 10). Therefore, contact cells play roles both in the propagation of JA-inducing electrical signals and in the synthesis of JA itself. However, a unique role of xylem in leaf-to-leaf SWP transmission in *Arabidopsis* is untenable. This means that a xylem stream-transported Ricca's factor does not function as a unique leaf-to-leaf wound signal in our experiments. Both of the *glr* double mutants that attenuate electrical signaling harbor the *glr3.3* mutation. Confirming a crucial role of the phloem in leaf-to-leaf electrical signal propagation, GLR3.3 is expressed in SEs, which are among the most excitable cells in the plant (15, 21). The activation of the jasmonate pathway powerfully affects plant growth (38), and therefore JA synthesis must be controlled tightly. A two-tissue mechanism of signal propagation may assure tight control over defense activation in tissues distal to wounds. In summary, rather than using a single extravascular cell population for organ-to-organ electrical signaling, the plant SWP co-opts two distinct cell types in the vascular matrix. This mode of electrical signaling involves parallel, nonadjacent cell files.

Membrane Potential Changes Precede Ca^{2+} Maxima. Several clade 3 GLRs localize to organelle membranes and/or to the plasma membrane (28–30, 39–41). Our results do not rigorously identify pools of active GLRs, and we do not rule out the existence of functional GLRs in the plasma membrane. However, in our study, pools of GLR-VENUS fusion proteins in leaves localized preferentially to the endoplasmic reticulum or to the vacuole. This is of interest because a hyperactive variant of a calcium-permeable vacuolar cation channel powerfully activated JA responses (22). How this occurs is unknown, but local changes in cytosolic Ca^{2+} concentration and/or Ca^{2+} uptake from the cytosol were among the hypotheses proposed to link intracellular cation/Ca^{2+} levels to JA synthesis activation (22). Moreover, SEs are sites of intense wound-response–associated calcium fluxes (17). Based on this, we simultaneously monitored cytosolic Ca^{2+} kinetics and electrical signals in leaves distal to wounds. By surgically removing extravascular tissues (Movie S2), we tested whether wound signals could be propagated through the primary vasculature. This was found to be the case for both Ca^{2+} signals and electrical signals. Therefore, signal propagation in leaves does not absolutely require extravascular cells. However, propagation of the calcium signal was delayed at the region of surgery. Either the integrity of the tissues surrounding the midvein helps to determine signal speed or epidermal GLR3.3 populations contribute to signal propagation.

A further finding was that each single *glr* mutant impacted the Ca^{2+} signal differently with *glr3.1* causing a bias in the radial distribution of the Ca^{2+} signal in the distal leaf. As with their impact on the electrical signal, the *glr3.1 glr3.3* and *glr3.3 glr3.6* double mutants strongly attenuated the distal calcium signal. We conclude that cytosolic calcium transients in response to wounding are regulated by several clade 3 GLRs and are strongly linked to the electrical signal. However, in the WT, GCaMP3 fluorescence maxima in leaves distal to wounds occurred on average 49 ± 8 s ($n = 7$) after the membrane depolarization maxima (e.g., Fig. 5*D*). How does this timing relate to JA accumulation in leaves distal to wounds? JA accumulation in leaves distal to wounds begins in the order of 90–120 s after wounding of distal leaves (9, 42). On average, it takes 66 s after wounding leaf 8 to initiate membrane depolarization in leaf 13 (3). Therefore, JA increases in the distal leaf lag behind the initial rapid depolarization phase of the SWP by at least 20 s. JA accumulation must therefore begin in or before the cytosolic Ca^{2+} maximum.

Comparison with Slow Wave Activities in Animals. Largely undefined at the cellular level, the plant SWP could not be readily compared with other electrical signaling phenomena in nature. However, the simultaneous monitoring of electrical signals and Ca^{2+} levels facilitates comparison of the SWP with electrical signaling phenomena found outside the plant kingdom. Such a comparison revealed several similarities to slow wave activities in

mammalian muscle such as that in the digestive system (43, 44): (*i*) rapid membrane depolarization and slow repolarization, (*ii*) centimeter-per-minute velocities of electrical signals, (*iii*) provocation of slow wave activity by current injection, and (*iv*) association with large and readily detectable cytosolic Ca^{2+} increases. While these parallels are intriguing, the mechanisms underlying plant and animal slow wave activities may differ since phloem and xylem are highly divergent from the cell populations involved in electrical signal propagation in metazoans. The deeper interest in clade 3 GLRs lies in the possibility that their study might yield novel insights into rapid communication between spatially separated cells.

Materials and Methods

All plants used were in the Col background. Generation of transgenics, complementation assays for GLR-VENUS fusions, insect bioassays, vein extraction, electrophysiology, and imaging procedures are documented in *SI Appendix, SI Materials and Methods*.

ACKNOWLEDGMENTS. We thank A. Lenglet for preparation of Fig. 3; The Lausanne Cellular Imaging Facility and, in particular, A. Paradis for support; N. Geldner for advice and access to microscopes; C. Darimont for providing insect eggs; S. Kellenberger for valuable discussion; and Christian Fankhauser for critical comments on the manuscript. This work was funded by Swiss National Science Foundation Grants 31003A-155960, 31003A-138235, 31003A-175566, and CRSII3 154438 (to E.E.F.).

1. Boari F, Malone M (1993) Wound-induced hydraulic signals: Survey of occurrence in a range of species. *J Exp Bot* 44:741–746.
2. Stahlberg R, Cleland RE, Van Volkenburgh E (2006) Slow wave potentials: A propagating electrical signal unique to higher plants. *Communication in Plants: Neuronal Aspects of Plant Life*, eds Baluška F, Mancuso S, Volkmann D (Springer, Heidelberg, Germany), pp 291–308.
3. Mousavi SA, Chauvin A, Pascaud F, Kellenberger S, Farmer EE (2013) GLUTAMATE RECEPTOR-LIKE genes mediate leaf-to-leaf wound signalling. *Nature* 500:422–426.
4. Farmer EE, Gasperini D, Acosta IF (2014) The squeeze cell hypothesis for the activation of jasmonate synthesis in response to wounding. *New Phytol* 204:282–288.
5. Choi WG, Hilleary R, Swanson SJ, Kim SH, Gilroy S (2016) Rapid, long-distance electrical and calcium signaling in plants. *Annu Rev Plant Biol* 67:287–307.
6. Browse J (2009) Jasmonate passes muster: A receptor and targets for the defense hormone. *Annu Rev Plant Biol* 60:183–205.
7. Chini A, Gimenez-Ibanez S, Goossens A, Solano R (2016) Redundancy and specificity in jasmonate signalling. *Curr Opin Plant Biol* 33:147–156.
8. Howe GA, Major IT, Koo AJ (2018) Modularity in jasmonate signaling for multistress resilience. *Annu Rev Plant Biol* 69:387–415.
9. Chauvin A, Caldelari D, Wolfender JL, Farmer EE (2013) Four 13-lipoxygenases contribute to rapid jasmonate synthesis in wounded *Arabidopsis thaliana* leaves: A role for lipoxygenase 6 in responses to long-distance wound signals. *New Phytol* 197:566–575.
10. Gasperini D, et al. (2015) Axial and radial oxylipin transport. *Plant Physiol* 169:2244–2254.
11. Houwink AL (1935) The conduction of excitation in *Mimosa pudica*. *Recl Trav Bot Neerl* 32:51–91.
12. Ricca U (1926) Transmission of stimuli in plants. *Nature* 117:654–655.
13. Evans MJ, Morris RJ (2017) Chemical agents transported by xylem mass flow propagate variation potentials. *Plant J* 91:1029–1037.
14. Stankovic B, Davies E (1998) The wound response in tomato involves rapid growth and electrical responses, systemically up-regulated transcription of proteinase inhibitor and calmodulin and down-regulated translation. *Plant Cell Physiol* 39:268–274.
15. Bose JC (1926) *The Nervous Mechanism of Plants* (Longmans Green, London), pp 224.
16. Rhodes JD, Thain JF, Wildon DC (1996) The pathway for systemic electrical signal conduction in the wounded tomato plant. *Planta* 200:50–57.
17. van Bel AJE, et al. (2014) Spread the news: Systemic dissemination and local impact of Ca^{2+} signals along the phloem pathway. *J Exp Bot* 65:1761–1787.
18. Hedrich R, Salvador-Recatalà V, Dreyer I (2016) Electrical wiring and long-distance plant communication. *Trends Plant Sci* 21:376–387.
19. Salvador-Recatalà V, Tjallingii WF, Farmer EE (2014) Real-time, in vivo intracellular recordings of caterpillar-induced depolarization waves in sieve elements using aphid electrodes. *New Phytol* 203:674–684.
20. Kiep V, et al. (2015) Systemic cytosolic $Ca^{(2+)}$ elevation is activated upon wounding and herbivory in *Arabidopsis*. *New Phytol* 207:996–1004.
21. Sibaoka T (1962) Excitable cells in Mimosa. *Science* 137:226.
22. Lenglet A, et al. (2017) Control of basal jasmonate signalling and defence through modulation of intracellular cation flux capacity. *New Phytol* 216:1161–1169.
23. Kurihara D, Mizuta Y, Sato Y, Higashiyama T (2015) ClearSee: A rapid optical clearing reagent for whole-plant fluorescence imaging. *Development* 142:4168–4179.
24. Ursache R, Andersen TG, Marhavý P, Geldner N (2018) A protocol for combining fluorescent proteins with histological stains for diverse cell wall components. *Plant J* 93:399–412.
25. Vincill ED, Clarin AE, Molenda JN, Spalding EP (2013) Interacting glutamate receptor-like proteins in phloem regulate lateral root initiation in *Arabidopsis*. *Plant Cell* 25:1304–1313.
26. Furch ACU, et al. (2009) Sieve element Ca^{2+} channels as relay stations between remote stimuli and sieve tube occlusion in *Vicia faba*. *Plant Cell* 21:2118–2132.
27. Geldner N, et al. (2009) Rapid, combinatorial analysis of membrane compartments in intact plants with a multicolor marker set. *Plant J* 59:169–178.
28. Kong D, et al. (2016) L-Met activates *Arabidopsis* GLR Ca^{2+} channels upstream of ROS production and regulates stomatal movement. *Cell Rep* 17:2553–2561.
29. Vincill ED, Bieck AM, Spalding EP (2012) $Ca^{(2+)}$ conduction by an amino acid-gated ion channel related to glutamate receptors. *Plant Physiol* 159:40–46.
30. Michard E, et al. (2011) Glutamate receptor-like genes form Ca^{2+} channels in pollen tubes and are regulated by pistil D-serine. *Science* 332:434–437.
31. Ortiz-Ramírez C, et al. (2017) GLUTAMATE RECEPTOR-LIKE channels are essential for chemotaxis and reproduction in mosses. *Nature* 549:91–95.
32. Tian L, et al. (2009) Imaging neural activity in worms, flies and mice with improved GCaMP calcium indicators. *Nat Methods* 6:875–881.
33. Vincent TR, et al. (2017) Interplay of plasma membrane and vacuolar ion channels, together with BAK1, elicits rapid cytosolic calcium elevations in *Arabidopsis* during aphid feeding. *Plant Cell* 29:1460–1479.
34. Castelfranco AM, Hartline DK (2016) Evolution of rapid nerve conduction. *Brain Res* 1641:11–33.
35. Wildon DC, et al. (1992) Electrical signaling and systemic proteinase-inhibitor induction in the wounded plant. *Nature* 360:62–65.
36. Manzoor H, et al. (2013) Involvement of the glutamate receptor AtGLR3.3 in plant defense signaling and resistance to *Hyaloperonospora arabidopsidis*. *Plant J* 76:466–480.
37. Fischer MC, et al. (2013) Population genomic footprints of selection and associations with climate in natural populations of *Arabidopsis halleri* from the Alps. *Mol Ecol* 22:5594–5607.
38. Huot B, Yao J, Montgomery BL, He SY (2014) Growth-defense tradeoffs in plants: A balancing act to optimize fitness. *Mol Plant* 7:1267–1287.
39. Teardo E, et al. (2011) Dual localization of plant glutamate receptor AtGLR3.4 to plastids and plasmamembrane. *Biochim Biophys Acta* 1807:359–367.
40. Teardo E, et al. (2015) Alternative splicing-mediated targeting of the *Arabidopsis* GLUTAMATE RECEPTOR3.5 to mitochondria affects organelle morphology. *Plant Physiol* 167:216–227.
41. Wudick MM, et al. (2018) CORNICHON sorting and regulation of GLR channels underlie pollen tube Ca^{2+} homeostasis. *Science* 360:533–536.
42. Glauser G, et al. (2009) Velocity estimates for signal propagation leading to systemic jasmonic acid accumulation in wounded *Arabidopsis*. *J Biol Chem* 284:34506–34513.
43. Angeli TR, et al. (2013) The bioelectrical basis and validity of gastrointestinal extracellular slow wave recordings. *J Physiol* 591:4567–4579.
44. Drumm BT, et al. (2017) Clustering of Ca^{2+} transients in interstitial cells of Cajal defines slow wave duration. *J Gen Physiol* 149:703–725.